International Journal of Advanced Trends in Engineering and Management (IJATEM)
Vol. 1(03), August 2022, pp. 1-10

Design of Polarization Reconfigurable Patch Antenna for Wireless Communications based on Fluidic Control Method

Y. Anlin Reena[1], E. Sree Devi[2]

[1]Department of Communication system, Rohini College of Engineering and Technology, Kanyakumari, India.
[2]Professor, Department of Communication system, Rohini College of Engineering and Technology, Kanyakumari, India.

ABSTRACT

Today's wireless communication systems heavily rely on polarization reconfigurable antennas because of the limitations on antenna orientation, increased channel capacity and removal of multipath interference. For wireless communications, it is therefore highly advantageous to construct such antennas. This project suggests a fluidic control method based circularly polarized patch antenna. The homogeneous substrate of a patch antenna is changed into an inhomogeneous substrate using ethyl acetate, a liquid dielectric. The creation of circularly polarized (CP) radiation occurs from two orthogonal excitations basic transverse magnetic (TM) modes by 90° phase difference. By adding liquid dielectric into various channels in substrate, proposed patch antenna's polarization may then be modified between right hand circular polarization (RHCP) as well as left hand circular polarization (LHCP). Considering W slot structure of radiating patch, proposed design exhibits three resonance frequencies.

Keywords: transverse magnetic (TM), left hand circular polarization (LHCP), circularly polarized (CP), right hand circular polarization (RHCP).

1 Introduction

Broad frequency range polarize reconfigurable pure water axial mode helical antenna [1]. Using pure water pumped into antenna's multiple chambers of Plexiglass holder, a water dielectric resonator antenna may function at the same operating frequency by switching between linear, RHCP and LHCP [2]. A maximum radiation efficiency over operational band of a circularly polarized (CP) water patch antenna was 48% [3]. The cavity backed slot antenna is able to continuously create stable unidirectional radiation patterns for all 20 states [4] by changing frequency, polarization and radiation pattern [3]. At a particular frequency range, a circular patch antenna with polarization reconfigurability may flip between circular polarizations that are left or right handed, vertically or horizontally [5].

A reconfigurable impedance converter and a quad polarization agile aperture coupled antenna could increase the 2.5% loss bandwidth [6]. High gain, consistent unidirectional radiation patterns and polarization reconfigurable cut ring micro strip antenna that can attain 10.0 dB for LP, RHCP as well as LHCP and over operational frequency spectrum [7]. The high gain of 6.9 dBic and the extraordinary stability of gain across whole bandwidth are achieved with L shaped feeding probes and a wideband circularly polarized reconfigurable patch antenna [8].The polarization reconfigurable glass DRA has a radiation efficiency and higher gain than majority of previously reported reconfigurable DRAs using P-I-N diodes, but advantage is offset by a slower reconfiguration speed [9]. In polarization agility antenna that employs liquid metal (eutectic gallium indium) and has a radiation efficiency of more than 90%, a substitute for silicon rubber that frequently tore out during injections has been found [10].

Liquid metal (LM) has to be improved, however the microfluidically frequency and polarization adjustable slot antenna has a very practical outlook on the design [11]. The suggested antenna is ideal for broadband usage in VHF band communications because at very high frequency (VHF) using broadband hybrid water antenna bands are stable within the targeted band [12]. The operational frequency range can see an increase in radiation efficiency from 15% - 52% to 84% using water antenna with coaxial dual tubes [13]. Low loss transformer oil patch antenna with frequency configurability (r=2.2) Due to the low loss transformer oil, this prototype exhibits remarkable radiation efficiency. The prototype also has a few appealing features, including frequency reconfigurability, a large adjustable range, good radiation efficiency, low cost and a straightforward structure [14].

Passively direct the radiation beam to the antenna concept in the appropriate fixed direction by taking advantage of the liquid's behavior as a result of gravity. This prototype doesn't somehow necessitate liquid pumps, tunable elements, phase shifting electrical power sources, or tunable components itself [15]. Modern wireless communication systems heavily rely on polarization reconfigurable antennas because to limits on antenna orientation, greater channel capacity and reduction of multipath interference. This makes it highly desirable to construct such antennas for wireless communications. Through a number of parametric studies, the performance characteristics have also been examined, adding considerably to design principles for future designs using several CP water patch antennas.

2 Proposed System

The usage of a compact, polarization adjustable patch antenna with a 2.357 GHz central frequency operating in 2.3 GHz range is advised. A W shaped slot is engraved on radiating patch. Switching the polarization type requires four tiny tactile switches (2mm x 3mm x 0.6mm). Tactile switches minimize the complexity and expense of fabricating antennas through doing away with requirement for biasing circuits. The beam width and cross polarization isolation of antenna are both satisfactory at 3 dB as well as better in working band. Any electromagnetic tool may be used to simulate antenna, which is constructed on FR4 substrate. With the use of W structure slots in radiating patch, the proposed design illustrates three resonance frequencies. It is suggested to use a rectangle MSA with W slot loading, inset feeding and four truncated corners on radiating patch's four corners. Using a network analyzer as well as an antenna radiation pattern test instrument, the antenna performance is validated. The measured results exhibit good agreement with predicted results when measured results are contrasted to other traditional approaches.

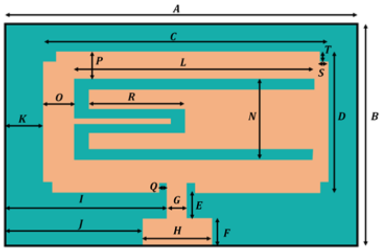

Figure 2.1 *Proposed block diagram*

2.1 Antenna Design

Figures 2.2 and 2.3 show the geometry and design of proposed electrically tiny rectangular Micro strip Patch antenna. Based on common designing process, the rectangular Micro strip patch antenna (RMPA) is built. The following equation provides antenna's length and breadth.

$$w = \frac{v_0}{2f_r}\sqrt{\frac{2}{\varepsilon_r+1}} \tag{1}$$

$$\varepsilon_{eff} = \frac{\varepsilon_r+1}{2} + \frac{\varepsilon_r-1}{2}\left[1+12\,\frac{h}{w}\right]^{-\frac{1}{2}} \tag{2}$$

$$\Delta L = 0.421h\,\frac{(\varepsilon_{eff}+0.3)(\frac{w}{h}+0.264)}{(\varepsilon_{eff}-0.258)(\frac{w}{h}+0.8)} \tag{3}$$

$$L = \frac{1}{2f_r\sqrt{\varepsilon_{eff}}\sqrt{\mu_0\varepsilon_0}} - 2\Delta L \tag{4}$$

Here, W stands for patch width, vo represents vacuum speed of light, r indicates substrate's dielectric constant, fr specifies target frequency, eff denotes dielectric constant of the material, L symbolizes a length extension of fringing effect, h expresses the thickness of substrate and L designates patch length.

Mathematical calculations of the parameters are followed by. The suggested antenna comprises a square patch with a modified W shaped slot that measures (WxL) 13mm x 13mm in size. With relative permittivity of 3.52 along with 1.5mm in thickness, low dielectric polymer weft yarn is used to print radiating patch on the surface. The suggested antenna's overall dimension structure is shown with the following measurements: w1 = 2mm, w2 = 4mm, w3 = 4mm, w4 = 3mm, w5 = 8mm and w6=6mm. The ground plane measures 22mm x 22mm and radiating patch is supplied via a coaxial probe at location shown in Figure 4.2.

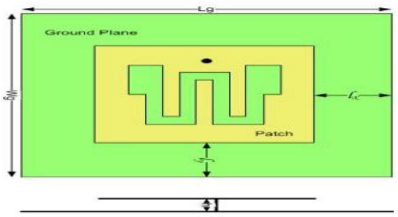

Figure. 2.2 *Geometry of proposed micro strip patch antenna*

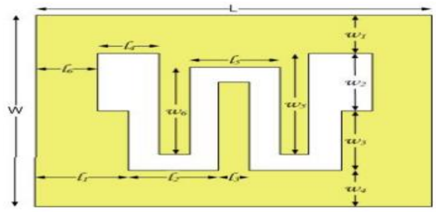

Figure. 2.3 *Different dimensions of proposed patch antenna*

Micro Strip Antennas are popular due to their desirable qualities, including low profile, cheap cost, simplicity, low weight of manufacture and integration with RF equipment and capacity to operate on several frequencies. It is common practice to employ linearly polarized micro strip antennas (LPMAs) in a variety of wireless communication applications. The single feed or dual feed types are the basis for categorizing LPMAs. Wideband single feed LPMAs are now getting a lot of attention. Due to its ability to excite polarization (LP) without the aid of external polarization, the single feed antenna is advantageous. For communication and radar systems including global positioning system (GPS) as well as synthetic aperture radar (SAR) use of dual frequency patch antennas has increased recently. By adding slots that are perpendicular to the patch co radiating axial's edges, dual frequency is obtained. Copper sheet was used to create patch radiator, which is then mounted on a glass epoxy base. This antenna's coaxial feed prevents it from being used in a low cost antenna array configuration. With the help of slot loading one can interact strongly between main patch and slot resonant frequency. The patch antenna's rectangular and slot loaded versions demonstrate that patch's slot cut has little effect on current distributions. A great way to improve and lessen impedance mismatch and a radiation pattern with almost same bandwidth is by slot loading.

3. Result and Discussion

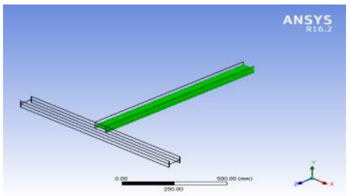

First Saved	Tuesday, July 19, 2022
Last Saved	Tuesday, July 19, 2022
Product Version	16.2 Release
Save Project Before Solution	No
Save Project After Solution	No

Figure 6.1: *ANSYS Software*

Figure 6.2: *Verification block*

Table 6.1

Unit System	Metric (mm, kg, N, s, mV, mA) Degrees rad/s Celsius
Angle	Degrees
Rotational Velocity	rad/s
Temperature	Celsius

Table 6.2: *Model (A4) > Geometry*

Object Name	*Geometry*
State	Fully Defined
Definition	
Source	C:\Users\Admin\Downloads\T SECTION.igs
Type	Iges
Length Unit	Meters
Element Control	Program Controlled
Display Style	Body Color
Bounding Box	
Length X	1000. mm
Length Y	50. mm
Length Z	1075. mm
Properties	
Volume	6.84e+005 mm³
Mass	5.3694 kg
Scale Factor Value	1.
Statistics	
Bodies	2
Active Bodies	2
Nodes	3720
Elements	544
Mesh Metric	None
Basic Geometry Options	
Solid Bodies	Yes
Surface Bodies	Yes
Line Bodies	No
Parameters	Yes
Parameter Key	DS
Attributes	No
Named Selections	No
Material Properties	No
Advanced Geometry Options	
Use Associativity	Yes
Coordinate Systems	No
Reader Mode Saves Updated File	No
Use Instances	Yes
Smart CAD Update	No
Compare Parts On Update	No
Attach File Via Temp File	Yes
Temporary Directory	C:\Users\Admin\AppData\Local\Temp
Analysis Type	3-D
Mixed Import Resolution	None
Decompose Disjoint Geometry	Yes
Enclosure and Symmetry Processing	Yes

Table 6. 3: Model *(A4) > Geometry > Parts*

Object Name	*Part 1*	*Part 2*
State	Meshed	
Graphics Properties		
Visible	Yes	
Transparency	1	
Definition		
Suppressed	No	
Stiffness Behavior	Flexible	
Coordinate System	Default Coordinate System	
Reference Temperature	By Environment	
Material		
Assignment	Structural Steel	
Nonlinear Effects	Yes	
Thermal Strain Effects	Yes	
Bounding Box		
Length X	1000. mm	75. mm
Length Y	50. mm	
Length Z	75. mm	1000. mm
Properties		
Volume	3.42e+005 mm³	
Mass	2.6847 kg	
Centroid X	65.059 mm	27.559 mm
Centroid Y	-22.642 mm	
Centroid Z	1037.5 mm	500. mm
Moment of Inertia Ip1	2887.9 kg·mm²	2.2405e+005 kg·mm²
Moment of Inertia Ip2	2.2629e+005 kg·mm²	
Moment of Inertia Ip3	2.2405e+005 kg·mm²	2887.9 kg·mm²
Statistics		
Nodes	1860	
Elements	272	
Mesh Metric	None	

Table 6.1, 6.2, 6.3, gives the details for geometry option for given modelling system.

International Journal of Advanced Trends in Engineering and Management (IJATEM)
Vol. 1(03), August 2022, pp. 1-10

Table 6.4: *Model (A4) > Coordinate Systems > Coordinate System*

Object Name	*Global Coordinate System*
State	Fully Defined
Definition	
Type	Cartesian
Coordinate System ID	0.
Origin	
Origin X	0. mm
Origin Y	0. mm
Origin Z	0. mm
Directional Vectors	
X Axis Data	[1. 0. 0.]
Y Axis Data	[0. 1. 0.]
Z Axis Data	[0. 0. 1.]

Table 6.4 shows the coordinate systems for the given modelling

Table 6.5: *Connections < Model (A4)*

Object Name	*Contacts*
State	Fully Defined
Definition	
Connection Type	Contact
Scope	
Scoping Method	Geometry Selection
Geometry	All Bodies
Auto Detection	
Tolerance Type	Slider
Tolerance Slider	0.
Tolerance Value	3.6726 mm
Use Range	No
Face/Face	Yes
Face/Edge	No
Edge/Edge	No
Priority	Include All
Group By	Bodies
Search Across	Bodies
Statistics	
Connections	1
Active Connections	1

Table 6.6: *Contacts <Connections <Model (A4)*

Object Name	*Connections*
State	Fully Defined
Auto Detection	
Generate Automatic Connection On Refresh	Yes
Transparency	
Enabled	Yes

Table 6.7: *Contact Regions < Contacts < Connections < Model (A4)*

Object Name	*Contact Region*
State	Fully Defined
Scope	
Scoping Method	Geometry Selection
Contact	1 Face
Target	1 Face
Contact Bodies	Part 1
Target Bodies	Part 2
Definition	
Type	Bonded
Scope Mode	Automatic
Behavior	Program Controlled
Trim Contact	Program Controlled
Trim Tolerance	3.6726 mm
Suppressed	No
Advanced	
Formulation	Program Controlled
Detection Method	Program Controlled
Elastic Slip Tolerance	Program Controlled
Thermal Conductance	Program Controlled
Pinball Region	Program Controlled
Geometric Modification	
Contact Geometry Correction	None
Target Geometry Correction	None

Table 6.5, 6.6, 6.7 shows the connections systems for the given modelling

Table 6.8: *Model (A4) > Mesh*

Object Name	*Mesh*
State	Solved
Display	
Display Style	Body Color
Defaults	
Physics Preference	Mechanical
Relevance	0
Sizing	
Use Advanced Size Function	Off
Relevance Center	Coarse
Element Size	Default
Initial Size Seed	Active Assembly
Smoothing	Medium
Transition	Fast
Span Angle Center	Coarse
Minimum Edge Length	2.0 mm
Inflation	
Use Automatic Inflation	None
Inflation Option	Smooth Transition
Transition Ratio	0.272
Maximum Layers	5
Growth Rate	1.2
Inflation Algorithm	Pre
View Advanced Options	No
Patch Conforming Options	
Triangle Surface Mesher	Program Controlled
Patch Independent Options	
Topology Checking	No
Advanced	
Number of CPUs for Parallel Part Meshing	Program Controlled
Shape Checking	Standard Mechanical
Element Midside Nodes	Program Controlled
Straight Sided Elements	No
Number of Retries	Default (4)
Extra Retries For Assembly	Yes
Rigid Body Behavior	Dimensionally Reduced
Mesh Morphing	Disabled
Defeaturing	
Pinch Tolerance	Please Define
Generate Pinch on Refresh	No
Automatic Mesh Based Defeaturing	On
Defeaturing Tolerance	Default
Statistics	
Nodes	3720
Elements	544
Mesh Metric	None

Table 6. 9: *Model (A4) > Analysis*

Object Name	*Steady-State Thermal (A5)*
State	Solved
Definition	
Physics Type	Thermal
Analysis Type	Steady-State
Solver Target	Mechanical APDL
Options	
Generate Input Only	No

Table 6.10: *Model (A4) > Steady State Thermal (A5) > Initial Condition*

Object Name	*Initial Temperature*
State	Fully Defined
Definition	
Initial Temperature	Uniform Temperature
Initial Temperature Value	22. °C

Table 6.11: *Model (A4) > Steady State Thermal (A5) > Analysis Settings*

Object Name	*Analysis Settings*
State	Fully Defined
Step Controls	
Number Of Steps	1.
Current Step Number	1.
Step End Time	1. s
Auto Time Stepping	Program Controlled
Solver Controls	
Solver Type	Program Controlled
Solver Pivot Checking	Program Controlled
Radiosity Controls	
Radiosity Solver	Program Controlled
Flux Convergence	1.e-004
Maximum Iteration	1000.
Solver Tolerance	1.e-007 W/mm^2
Over Relaxation	0.1
Hemicube Resolution	10.
Nonlinear Controls	
Heat Convergence	Program Controlled
Temperature Convergence	Program Controlled
Line Search	Program Controlled
Output Controls	
Calculate Thermal Flux	Yes
General Miscellaneous	No
Store Results At	All Time Points
Analysis Data Management	
Solver Files Directory	C:\Users\Admin\AppData\Local\Temp\WB_ABT4_Admin_8156_2\unsaved_project_files\dp0\SYS\MECH\
Future Analysis	None
Scratch Solver Files Directory	
Save MAPDL db	No
Delete Unneeded Files	Yes
Nonlinear Solution	No
Solver Units	Active System
Solver Unit System	nmm

Table 6.11 shows the analysis setting of the given project.

Table 6.12: *Loads < Steady State Thermal (A5) < Model (A4)*

Object Name	*Temperature*	*Heat Flow*
State	Fully Defined	
Scope		
Scoping Method	Geometry Selection	
Geometry	1 Face	2 Faces
Definition		
Type	Temperature	Heat Flow
Magnitude	22. °C (ramped)	200. W (ramped)
Suppressed	No	

Table 6.13: *Solution < Steady State Thermal (A5) < Model (A4)*

Object Name	*Total Heat Flux*	*Directional Heat Flux*
State	Solved	
Scope		
Scoping Method	Geometry Selection	
Geometry	All Bodies	
Definition		
Type	Total Heat Flux	Directional Heat Flux
By	Time	
Display Time	Last	
Calculate Time History	Yes	
Identifier		
Suppressed	No	
Orientation		X Axis
Coordinate System		Global Coordinate System
Integration Point Results		
Display Option	Averaged	
Average Across Bodies	No	
Results		
Minimum	9.4794e-010 W/mm^2	-0.63952 W/mm^2
Maximum	0.65009 W/mm^2	0.49562 W/mm^2
Minimum Occurs On	Part 2	Part 1
Maximum Occurs On	Part 1	Part 2
Information		
Time	1. s	
Load Step	1	
Substep	1	
Iteration Number	1	

Figure 6.3: *Temperature < Steady State Thermal (A5) < Model (A4)*

Figure 6.4: *Heat Flow < Steady State Thermal (A5) < Model (A4)*

Table 6.14: *Solution Information < Solution (A6) < Steady State Thermal (A5) <Model (A4)*

Object Name	*Solution (A6)*
State	Solved
Adaptive Mesh Refinement	
Max Refinement Loops	1.
Refinement Depth	2.
Information	
Status	Done
Post Processing	

International Journal of Advanced Trends in Engineering and Management (IJATEM)
Vol. 1(03), August 2022, pp. 1-10

Table 6.15: *Results < Solution (A6) < Steady State Thermal (A5) < Model (A4)*

Object Name	*Solution Information*
State	Solved
Solution Information	
Solution Output	Solver Output
Update Interval	2.5 s
Display Points	All
FE Connection Visibility	
Activate Visibility	Yes
Display	All FE Connectors
Draw Connections Attached To	All Nodes
Line Color	Connection Type
Visible on Results	No
Line Thickness	Single
Display Type	Lines

Table 6.13, 6.14, 6.15, shows the solutions and results at steady state condition of the given object.

Figure 6.5: *Model (A4) > Steady State Thermal (A5) > Solution (A6) > Total Heat Flux*

Table 6.16: *Model (A4) > Steady State Thermal (A5) > Solution (A6) > Total Heat Flux*

Time [s]	Minimum [W/mm²]	Maximum [W/mm²]
1.	9.4794e-010	0.65009

Figure 6.6 *Model (A4) > Steady State Thermal (A5) > Solution (A6) > Directional Heat Flux*

Table 6.17: *Model (A4) > Steady State Thermal (A5) > Solution (A6) > Directional Heat Flux*

Time [s]	Minimum [W/mm²]	Maximum [W/mm²]
1.	-0.63952	0.49562

Table 6.18: *Constants < Structural Steel*

Density	7.85e-006 kg mm^-3
Coefficient of Thermal Expansion	1.2e-005 C^-1
Specific Heat	4.34e+005 mJ kg^-1 C^-1
Thermal Conductivity	6.05e-002 W mm^-1 C^-1
Resistivity	1.7e-004 ohm mm

TABLE 6.19: *Structural Steel > Compressive Ultimate Strength*

Compressive Ultimate Strength MPa
0

TABLE 6.20: *Structural Steel > Compressive Yield Strength*

Compressive Yield Strength MPa
250

TABLE 6.21: *Structural Steel > Tensile Yield Strength*

Tensile Yield Strength MPa
250

TABLE6.22: *Structural Steel > Tensile Ultimate Strength*

Tensile Ultimate Strength MPa
460

TABLE 6. 23: *Structural Steel > Isotropic Secant Coefficient of Thermal Expansion*

Reference Temperature C
22

Table 6. 24: *Alternating Stress Mean Stress < Structural Steel*

Alternating Stress MPa	Cycles	Mean Stress MPa
3999	10	0
2827	20	0
1896	50	0
1413	100	0
1069	200	0
441	2000	0
262	10000	0
214	20000	0
138	1.e+005	0
114	2.e+005	0
86.2	1.e+006	0

Table 6.25: *Strain Life Parameters< Structural Steel*

Strength Coefficient MPa	Strength Exponent	Ductility Coefficient	Ductility Exponent	Cyclic Strength Coefficient MPa	Cyclic Strain Hardening Exponent
920	-0.106	0.213	-0.47	1000	0.2

Table 6. 26: *Isotropic Elasticity< Structural Steel*

Temperature C	Young's Modulus MPa	Poisson's Ratio	Bulk Modulus MPa	Shear Modulus MPa
	2.e+005	0.3	1.6667e+005	76923

Table 6.27: *Isotropic Relative Permeability < Structural Steel*

Relative Permeability
10000

4. Conclusion

The coaxial feed, linearly polarized, w slot loaded micro strip antenna design and simulation are accomplished. An antenna with coaxial feed and a rectangular slot loaded micro strip is recommended for polarization. By putting in rectangular slot, the antenna can easily become more compact. Following simulation, it was determine that antenna's return loss was less than -10 dB, making it suitable for usage in real world applications. Theoretical and practical results are verified using equivalent circuit topology described in the proposed work.

References

1. Ren Zhen; Shi-Shan Qi; Zhenxin Hu; Zhong Xiang Shen; Wen Wu, Year: 2019, "Wideband water helical antenna of circular polarization", IEEE Transactions on Antennas and Propagation, Vol: 67, no: 11, pp: 6770–6777.

2. Wang Min; Qing-Xin Chu, Year: 2019, "A wideband polarization-reconfigurable water dielectric resonator antenna," IEEE Antennas and Wireless Propagation Letters, Vol: 18, pp: 402–406.

3. Sun Jie; Kwai-Man Luk, Year: 2020, "A circularly polarized water patch antenna", IEEE Antennas and Wireless Propagation Letters, Vol: 19, pp: 926–929.

4. Ge Lei; Yujian Li; Jianpeng Wang, Year: 2017, "A low-profile reconfigurable cavity-backed slot antenna with frequency, polarization and radiation pattern agility" IEEE Transactions on Antennas and Propagation, Vol: 65, no: 05, pp: 2182–2189.

5. Mak Ka Ming; Hau Wah Lai; Kwai Man Luk; Kin Lun Ho, Year: 2017, "Polarization reconfigurable circular patch antenna with a C-shaped", IEEE Transactions on Antennas and Propagation, Vol: 65, no: 03, pp: 1388–1392.

6. Sun Hucheng; Zhiqiang Pan, Year: 2019, "Design of a quad-polarization-agile antenna using a switchable impedance converter", IEEE Antennas and Wireless Propagation Letters, Vol: 18, pp: 269–273.

7. Chen Qingqing; Jian-ying Li; Guangwei Yang; Bao Cao; Zhaolin Zhang, Year: 2019, "A polarization reconfigurable high-gain micro strip antenna", IEEE Transactions on Antennas and Propagation, Vol: 67, no: 05, pp: 3461–3466.

8. Lin,Wei; Hang Wong, Year: 2017, "Wideband circular-polarization reconfigurable antenna with L-shaped feeding probes", IEEE Antennas and Wireless Propagation Letters, Vol: 16, pp: 2114–2117.

9. Chen Zhe; Hang Wong; James Kelly, Year: 2019, "A polarization-reconfigurable glass dielectric resonator antenna using liquid metal", IEEE Transactions on Antennas and Propagation, Vol: 67, no: 05, pp: 3427–3432.

10. Wang Cong; Joo Chuan Yeo; Hui Chu; Chwee Teck Lim; Yong-Xin Guo, Year: 2018, "Design of a reconfigurable patch antenna using the movement of liquid metal", IEEE Antennas and Wireless Propagation Letters, Vol: 17, pp: 974–977, 2018.

11. Liu Ying; Qia Wang; Yongtao Jia; Peisheng Zhu, Year: 2020, "A frequency- and polarization reconfigurable slot antenna using liquid metal", IEEE Transactions on Antennas and Propagation, Vol: 68, no: 11, pp: 7630–7635.

12. Qian Ya-Hui; Qing-Xin Chu, Year: 2017, "A broadband hybrid monopole-dielectric resonator water antenna", IEEE Antennas and Wireless Propagation Letters, Vol: 16, pp: 360–363, 2017.

13. Wang Min; Qing-Xin Chu, Year: 2018, "High-efficiency and wideband coaxial dual-tube hybrid monopole water antenna", IEEE Antennas and Wireless Propagation Letters, Vol: 17, pp: 799–802.

14. Wang Shiyan; Lei Zhu; Wen Wu, Year: 2017, "A novel frequency-reconfigurable patch antenna using low-loss transformer oil", IEEE Transactions on Antennas and Propagation, Vol: 65, no: 12, pp: 7316–7321.

15. Song Chaoyun; Elliot L. Bennett; Jianliang Xiao; Tianyuan Jia; Rui Pei; Kwai-Man Luk; Yi Huang, Year: 2020, "Passive beam-steering gravitational liquid antennas", IEEE Transactions on Antennas and Propagation, Vol: 68, no: 04, pp: 3207–3212.